Structure and Physical Properties of $(EP\text{-}TTP)_2Au(CN)_2$

Takehiko MORI,* Yohji MISAKI,*,† and Tokio YAMABE†
Department of Organic and Polymeric Materials, Tokyo Institute of Technology, O-okayama, Meguro-ku, Tokyo 152
† Division of Molecular Engineering, Graduate School of Engineering, Kyoto University, Yoshida, Kyoto 606
(Received June 6, 1994)

The title organic charge transfer salt, where EP-TTP is 2-(4,5-ethylenedithio-1,3-dithiol-2-ylidene)-5-(4,5-trimethylenedithio-1,3-dithiol-2-ylidene)-1,3,4,6-tetrathiapentalene, has so-called β-type donor arrangement, but the Fermi surface is basically one-dimensional. This salt exhibits metallic conductivity down to 0.7 K. The thermoelectric power and ESR show simple metal-like behavior.

A new series of organic donors, bis-fused tetrathiafulvalenes (TTF), have afforded a number of highly conducting radical-cation salts that maintain metallic conductivity down to liquid helium temperatures.[1] The main obstacle to preparing salts of these donors is, however, poor solubility of these donors in organic solvents; this makes the conventional electrochemical crystal growth difficult. In particular, "capped" moieties such as ethylenedithio group considerably diminish the solubility. Unsymmetrical substitution, however, considerably improve the solubility. For example, 2-(4,5-ethylenedithio-1,3-dithiol-2-ylidene)-5-(4,5-trimethylenedithio-1,3-dithiol-2-ylidene)-1,3,4,6-tetrathiapentalene (hereafter abbreviated symbolically as EP-TTP, Scheme 1) shows a little better solubility than its symmetrical analogs. Because fairly good crystals of its $[Au(CN)_2]^-$ salt was obtained and showed metallic conductivity down to low temperatures, the present paper describes the results of its single-crystal structure analysis, energy-band calculation, electrical conductivity, thermoelectric power, and ESR measurements.

Experimental

Black needle-like crystals were electrochemically grown in 1,1,2-trichloroethane, tetrahydrofuran, or benzonitrile in the presence of the donor[1] and tetrabutylammonium dicyanoaurate(I).[2] Intensity data of single crystal X-ray structure analysis were measured at 298 K for a single crystal with approximate dimensions $0.8\times0.01\times0.08$ mm^3 by the ω–2θ scan technique on a Rigaku automated four-circle diffractometer AFC-5R with graphite monochromatized Mo $K\alpha$ ($\lambda=0.7103$ Å) radiation ($2\theta<55°$). Crystallographic data: $C_{32}H_{20}N_2S_{24}Au$, $M=1399.075$, triclinic, space group $P\bar{1}$, $a=8.916(3)$, $b=17.916(7)$, $c=7.944(4)$ Å, $\alpha=101.74(4)$, $\beta=112.28(3)$, $\gamma=82.33(3)°$, $V=1147.5(9)$ Å^3, $Z=1$, $D_c=2.025$ g cm^{-1}, and μ(Mo $K\alpha$)$=42.84$ cm^{-1}. The structure was solved by the direct method[3] and was refined by the block-diagonal least-squares procedure (UNICS III).[4] The atomic scattering factors were taken from the "International Tables for X-Ray Crystallography".[5] Anisotropic thermal parameters were adopted for all non-hydrogen atoms, and the hydrogen atoms were refined isotropically. The final $R=0.105$ and $R_w=0.092$ (weighting scheme $1/w=\sigma^2+(0.015F_o)^2$ for independent 1483 reflections ($|F_o|>3\sigma(F_o)$).[6]

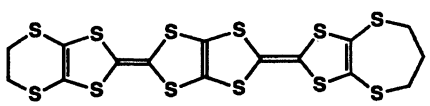

EP-TTP

Scheme 1.

The electrical conductivity was measured by the conventional four-probe method with low-frequency (80 Hz) alternating current. The electrical contacts were made with gold paint.

The thermoelectric power was measured by attaching a sample to two copper heat blocks with gold foil and gold paint. The heat blocks were alternately heated to generate a temperature gradient of about 0.2—0.5 K. The generated electromotive forces of the sample and of the differential thermocouple were measured by two microvoltmeters and processed on a microcomputer.

The ESR spectra were measured with a Varian Associates X-band E112 spectrometer. The temperature control was achieved using an Oxford Instruments ESR9 continuous-flow helium cryostat. The magnetic field was applied approximately along the crystallographic c axis. The g-value was almost temperature independent ($g=2.020$).

Results and Discussion

The atomic coordinates and equivalent thermal parameters are listed in Table 1. Atomic numbering scheme of the donor is shown in Fig. 1(a). One EP-TTP molecule is crystallographically independent, whereas $Au(CN)_2$ lies on an inversion center, implying the composition to be $(EP\text{-}TTP)_2Au(CN)_2$. This is consistent with the chemical analysis by means of the energy dispersion spectroscopy, which shows, from the ratio of S and Au, EP-TTP : $Au(CN)_2$ to be 1 : 0.497.

The EP-TTP molecule is basically planar except the terminal ethylene and trimethylene carbons; the deviations from the optimal plane are within 0.1 Å. Similarly to other 2 : 1 cation radical salts, the donors and the anions form segregated layers which are alternately stacked along the crystallographic b axis (Fig. 2).

In the donor sheet, the donor molecules makes a face-to-face stack along the [101] direction (Fig. 3), in which the ethylene and the trimethylene parts are arranged alternately. Therefore there is no disorder originating from the unsymmetry of the donor molecule.

This donor arrangement has a close resemblance to the well-known β-$(BEDT\text{-}TTF)_2I_3$ (BEDT-TTF: bis(ethylenedithio)tetrathiafulvalene).[7] Table 2 lists the

Table 1. Atomic Coordinates ($\times 10^4$) and Equivalent Isotropic Thermal Parameters of (EP-TTP)$_2$Au(CN)$_2$

Atom	x	y	z	B_{eq}[a)]/Å
Au	0	0	0	4.0
C	1018(53)	356(50)	2765(53)	20.1
N	1606(45)	470(26)	4247(45)	10.5
S(1)	7570(11)	8057(5)	12998(11)	3.8
S(2)	9428(10)	7152(6)	9987(12)	3.8
S(3)	5101(9)	6906(5)	11051(11)	2.9
S(4)	6681(10)	6162(5)	8434(11)	2.8
S(5)	2371(10)	5661(5)	9280(11)	2.8
S(6)	4018(10)	4896(5)	6680(11)	2.9
S(7)	−287(10)	4524(5)	7450(11)	2.7
S(8)	1388(10)	3760(5)	4872(11)	2.8
S(9)	−2981(10)	3227(5)	5569(11)	3.1
S(10)	−1305(10)	2531(5)	3013(11)	3.4
S(11)	−5516(11)	2092(6)	4051(12)	3.8
S(12)	−3652(11)	1341(5)	985(12)	3.9
C(1)	8771(66)	8506(24)	12156(68)	11.2
C(2)	9657(41)	8081(25)	11059(62)	7.4
C(3)	6904(36)	7258(16)	11354(37)	2.4
C(4)	7641(32)	6922(14)	10075(38)	2.1
C(5)	5093(36)	6144(17)	9207(38)	2.7
C(6)	3993(33)	5652(15)	8530(39)	2.2
C(7)	1539(31)	4876(17)	7706(38)	2.4
C(8)	2242(35)	4556(17)	6510(36)	2.5
C(9)	−251(29)	3748(18)	5609(34)	2.6
C(10)	−1384(29)	3298(19)	4789(40)	3.4
C(11)	−3775(31)	2416(17)	3938(37)	2.3
C(12)	−3033(33)	2117(16)	2777(35)	2.4
C(13)	−4872(36)	1160(17)	4499(43)	3.3
C(14)	−4777(42)	537(20)	2907(49)	4.8
C(15)	−3368(42)	555(16)	2262(44)	4.0

a) $B_{eq}=4/3(\sum_i \sum_j B_{ij} \boldsymbol{a}_i \cdot \boldsymbol{a}_j)$

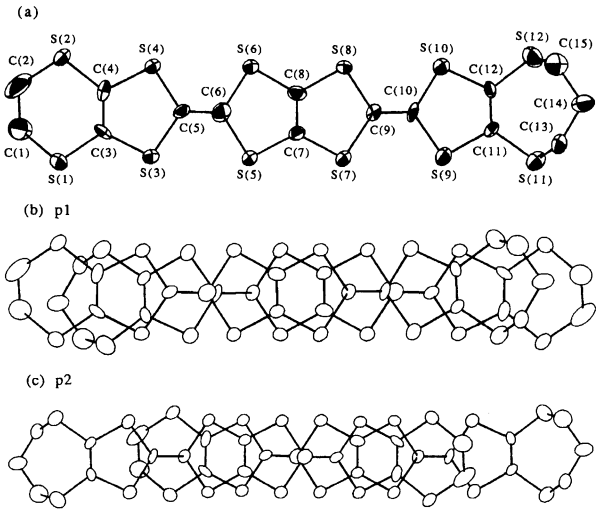

Fig. 1. (a) Atomic numbering scheme of EP-TTP, intrastack overlap mode of p1 (b) and p2 (c).

comparison of the present salt and β-(BEDT-TTF)$_2$I$_3$, where S is the intermolecular overlap integrals of the HOMO of the adjacent molecules,[8] ϕ is the angle of the intermolecular vector from the molecular plane, and D is the slip distance along the molecular long axis. Along the stacking direction, D is 1.7 Å for p1 and 4.7 Å for p2. Because the length of one dithiole ring is about 3.2 Å, these D's mean that the slips correspond respectively half and one and half units of the dithiole rings. Therefore the overlap mode is so-call ring-over-bond type in both cases as shown in Fig. 1(b) and (c). The intermolecular interaction S is, however, not sensitive to D.[8] The large difference of the p1 and p2 interactions in β-(BEDT-TTF)$_2$I$_3$ instead comes from the difference of the interplanar spacings: 3.39 Å for p1 and 3.98 Å for p2. This strong dimerization has been attributed to the steric effect of the terminal out-of-plane ethylene carbons.[7] On the contrary the interplanar distances in (EP-TTP)$_2$Au(CN)$_2$ are 3.52 Å (p1) and 3.47 Å (p2); the dimerization is very weak, resulting in the approximately same magnitude of the p1 and p2 interactions. The large slip distance D=4.7 Å in (EP-TTP)$_2$Au(CN)$_2$ may be also related to avoiding the steric hindrance of the terminal groups. It is noteworthy that in EP-TTP, because the molecule size is much larger, the large D does not diminish the overlap interaction S.

The interstack interactions of (EP-TTP)$_2$Au(CN)$_2$ is about one fifth to one sixth of the intrastack interac-

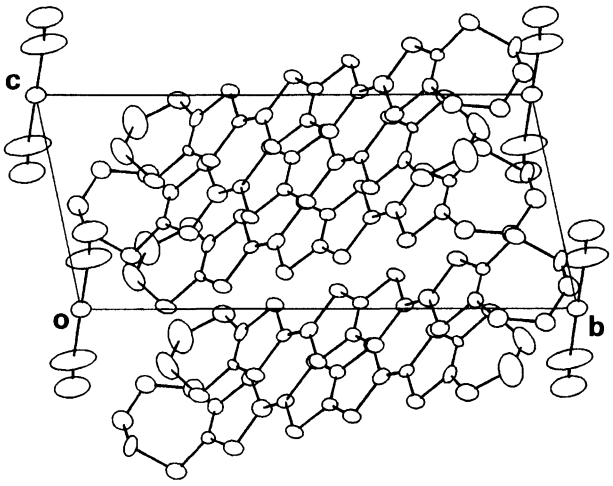

Fig. 2. Crystal structure of (EP-TTP)$_2$Au(CN)$_2$, viewed along the a axis.

Table 2. Intermolecular Overlap Integrals of the HOMO, S, and the Parameters ϕ and D Which Define the Orientation of Neighboring Molecules (see text) in (EP-TTP)$_2$Au(CN)$_2$ and β-(BEDT-TTF)$_2$I$_3$

	(EP-TTP)$_2$Au(CN)$_2$			β-(BEDT-TTF)$_2$I$_3$		
	$S\times10^{-3}$	ϕ/°	D/Å	$S\times10^{-3}$	ϕ/°	D/Å
p1	−17.6	90	1.7	−24.5	87	1.5
p2	−24.5	88	4.7	−8.4	84	3.8
q1	−3.1	12	4.4	−12.7	22	2.0
q2	−0.6	20	6.0	−6.8	18	0.3
a	−4.4	11	1.4	−5.0	14	1.8

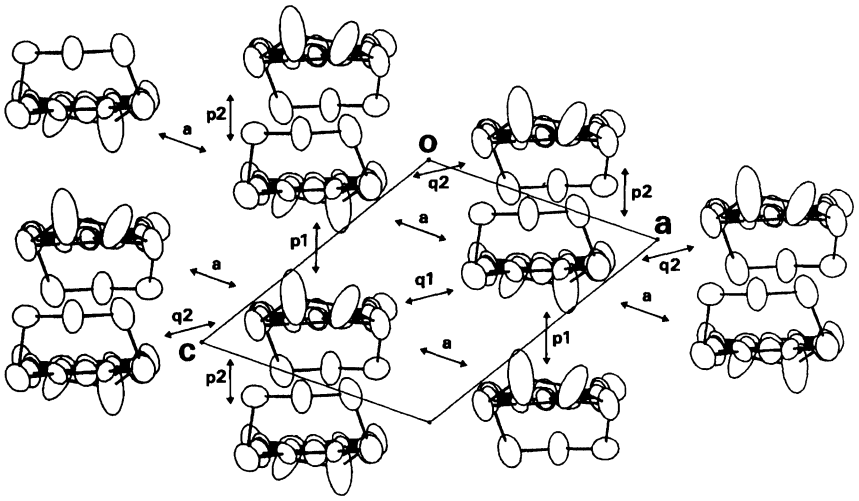

Fig. 3. Donor arrangement of (EP-TTP)$_2$Au(CN)$_2$, viewed along the donor long axis.

tions. This is in striking contrast to β-(BEDT-TTF)$_2$I$_3$, where the interstack interactions are not much different from the intrastack interactions. It should be also noted that D's of the interstack interactions are rather large in (EP-TTP)$_2$Au(CN)$_2$ (Table 2), suggesting a basically different donor arrangements between β-(BEDT-TTF)$_2$I$_3$ and (ET-TTP)$_2$Au(CN)$_2$. As a result, the tight-binding band structure, calculated from these S, is rather one-dimensional in (EP-TTP)$_2$Au(CN)$_2$ (Fig. 4); though the feature around the B point is somewhat tricky, the calculated Fermi surface is open perpendicularly to the stacking direction. In spite of the apparent resemblance of the donor arrangement, the comparatively small interstack interactions as well as the weak dimerization make (EP-TTP)$_2$Au(CN)$_2$ rather one-dimensional.

Because the crystals were elongated along the crystallographic [101] direction, which corresponds to the stacking direction, the electrical conductivity was measured along this direction (Fig. 5). The room-temperature conductivity is about 400 S cm^{-1} and metal-like down to liquid helium temperatures. The resistivity is approximately proportional to T^2. The resistivity decreased to 1/17 of the room-temperature value, but superconductivity was not observed down to 0.7 K, the lowest measured temperature.

The thermoelectric power (Seebeck coefficient) along

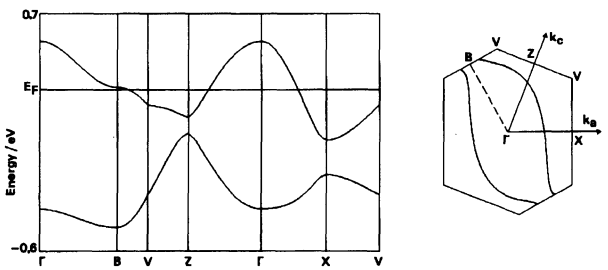

Fig. 4. Tight-binding energy band structure and Fermi surface of (EP-TTP)$_2$Au(CN)$_2$.

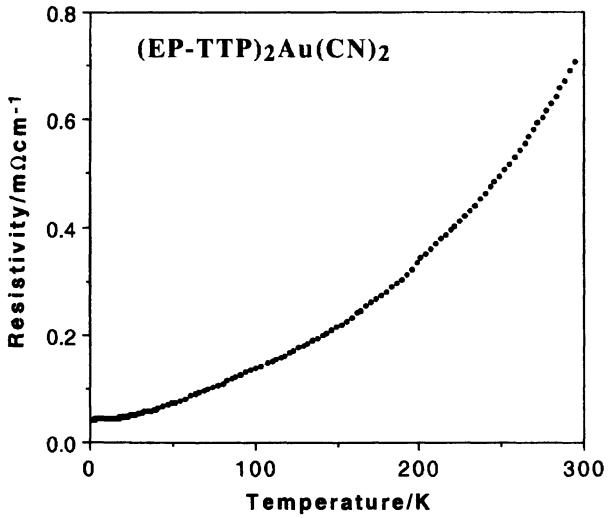

Fig. 5. Electrical resistivity of (EP-TTP)$_2$Au(CN)$_2$, measured along the needle axis (//[101]).

the [101] direction is shown in Fig. 6. The thermoelectric power is positive and T-linear in the whole temperature range, agreeable with a simple donor conductor. A small hump around 60 K is probably related to phonon drag. Two-dimensional conductors such as BETD-TTF salts show complicated temperature dependence, but ordinary one-dimensional conductors show simple T-linear behavior.[9] Therefore the observed T-linear dependence of the present salt may be related to the aforementioned basically one-dimensional energy band. The thermoelectric power of a tight-binding one-dimensional band is given as:

$$S = \frac{\pi^2 k_B^2 T}{6et} \frac{\cos(1/2\pi\rho)}{1-\cos^2(1/2\pi\rho)}. \quad (1)$$

From this relation, the gradient of the observed thermoelectric power gives the bandwidth of $4t$=0.67 eV. This value is basically consistent with the calculated band structure (Fig. 4), and is almost the same as the

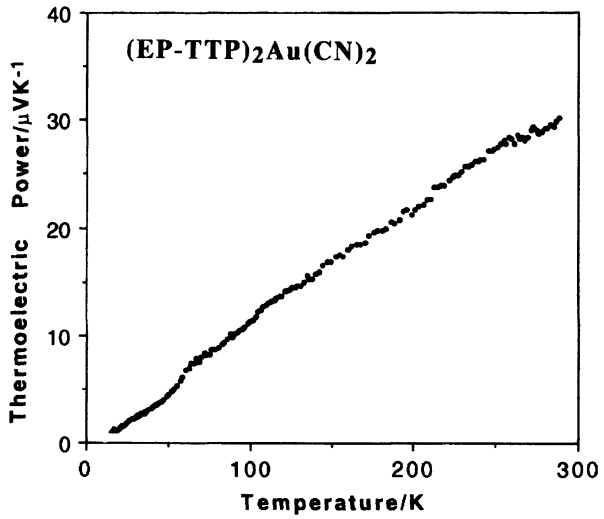

Fig. 6. Thermoelectric power of $(EP\text{-}TTP)_2Au(CN)_2$, measured along the needle axis (//[101]).

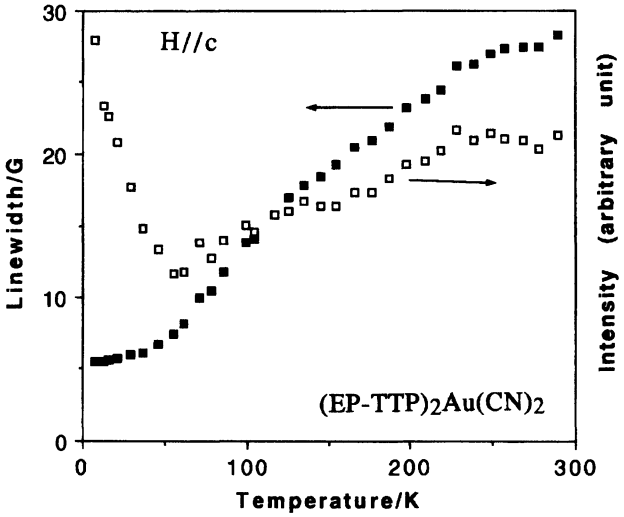

Fig. 7. ESR peak-to-peak linewidth and intensity of $(EP\text{-}TTP)_2Au(CN)_2$.

values of the ordinary organic conductors.

The ESR peak-to-peak linewidth and intensity are shown in Fig. 7. The approximately T-linear dependence of the linewidth is consistent with the metallic conduction. Though the ESR intensity, which should be proportional to the spin susceptibility, slightly decreases with lowering the temperature, it basically indicates the Pauli-like T-independent susceptibility (because it at least does not show Curie-like increase). Below 50 K the influence of impurities seems to be important. The room-temperature linewidth 28 G is rather narrow in comparison with BEDT-TTF salts,[10] suggesting comparatively one-dimensional Fermi surface of the present salt.

In conclusion from the viewpoint of the crystal structure and the band calculation we have discussed the comparatively one-dimensional electronic structure of $(EP\text{-}TTP)_2Au(CN)_2$ in spite of the apparent resemblance of the donor arrangement to that of β-$(BEDT\text{-}TTF)_2I_3$. The results of thermoelectric power and ESR seem to support this conclusion. Though the Fermi surface is open, the interstack interactions seem to be large enough to suppress the possible one-dimensional instability. As a result, the present salt exhibits a quite simple "metal-like" behavior down to low temperatures. It may be not surprising that EP-TTP shows more one-dimensional character than BEDT-TTF, because BPDT-TTF (bis(trimethylenedithio)tetrathiafulvalene) salts have been known to show highly one-dimensional properties.[11] The present investigation demonstrates sensitivity of the physical properties to the molecular design, and necessity of the further endeavor of materials design even in the framework of the bis-fused TTF series.

References

1) Y. Misaki, H. Nishikawa, T. Yamabe, T. Mori, H. Inokuchi, H. Mori, and S. Tanaka, *Chem. Lett.*, **1993**, 729, 733, 2073, and 2085; *Bull. Chem. Soc. Jpn.*, **67**, 661 (1994).

2) P. J. Nigrey, B. Morosin, J. F. Kwak, E. L. Venturini, and R. J. Baughman, *Synth. Metals*, **16**, 1 (1986).

3) G. M. Sheldric, "Crystallographic Computing 3," Oxford University Press, Oxford II (1985), pp. 175—189.

4) T. Sakurai and K. Kobayashi, *Rep. Inst. Phys. Chem. Res.*, **55**, 69 (1979).

5) "International Tables for X-Ray Crystallography," Kynoch Press, Birmingham (1974), Vol. IV.

6) The structure factor table and the list of anisotropic thermal parameters are deposited as Document No. 67075 at the Office of the Editor of Bull. Chem. Soc. Jpn.

7) T. Mori, A. Kobayashi, Y. Sasaki, H. Kobayashi, G. Saito, and H. Inokuchi, *Chem. Lett.*, **1984**, 957.

8) T. Mori, A. Kobayashi, Y. Sasaki, H. Kobayashi, G. Saito, and H. Inokuchi, *Bull. Chem. Soc. Jpn.*, **57**, 627 (1984).

9) T. Mori and H. Inokuchi, *J. Phys. Soc. Jpn.*, **57**, 3674 (1988).

10) J. M. Williams, J. R. Ferraro, R. J. Thorn, K. D. Carlson, U. Geiser, H. H. Wang, A. M. Kini, and M. -H. Whangbo, "Organic Superconductors," Prentice Hall, New Jersey (1992), p. 189.

11) R. Kato, T. Mori, A. Kobayashi, Y. Sasaki, and H. Kobayashi, *Chem. Lett.*, **1984**, 781 and 1335.